


Co-expression analysis aids in the identification of genes in the cuticular wax pathway in maize

Jun Zheng^{1,*} , Cheng He^{2,*}, Yang Qin¹, Guifang Lin², Woojun D. Park^{2,†}, Minghao Sun^{1,3}, Jian Li^{1,3}, Xiaoduo Lu⁴, Chunyi Zhang⁵, Cheng-Ting Yeh⁶, Chathura J. Gunasekara⁷, Erliang Zeng^{8,9}, Hairong Wei^{10,11}, Patrick S. Schnable^{6*}, Guoying Wang^{1*} and Sanzhen Liu^{2*}

¹Institute of Crop Sciences, Chinese Academy of Agricultural Sciences, Beijing 100081, China,

²Department of Plant Pathology, Kansas State University, Manhattan, KS 66506, USA,

³College of Agronomy, Jilin Agricultural University, Changchun, Jilin 130118, China,

⁴Institute of Molecular Breeding for Maize, Qilu Normal University, Jinan 250200, China,

⁵Biotechnology Research Institute, Chinese Academy of Agricultural Sciences, Beijing 100081, China,

⁶Department of Agronomy, Iowa State University, Ames, IA 50011-3605, USA,

⁷USDA/ARS Children's Nutrition Research Center, Department of Pediatrics, Baylor College of Medicine, Houston, TX, USA,

⁸Division of Biostatistics and Computational Biology, College of Dentistry, University of Iowa, Iowa City, IA 52242, USA,

⁹Department of Biostatistics, University of Iowa, Iowa City, IA 52242, USA,

¹⁰Beijing Advanced Innovation Center for Tree Breeding by Molecular Design, Beijing Forestry University, Beijing 100083, China, and

¹¹School of Forest Resources and Environmental Science, Michigan Technological University, Houghton, MI 49931, USA

Received 16 August 2018; revised 9 October 2018; accepted 22 October 2018.

*For correspondence (e-mails schnable@iastate.edu, wangguoying@caas.cn, liuzhen@ksu.edu).

†Present address: Department of Molecular and Human Genetics, Baylor College of Medicine, Houston, TX, USA.

‡These authors contributed equally to this work.

SUMMARY

Epicuticular waxes provide a hydrophobic barrier that protects land plants from environmental stresses. To elucidate the molecular functions of maize glossy mutants that reduce the accumulation of epicuticular waxes, eight non-allelic glossy mutants were subjected to transcriptomic comparisons with their respective wild-type siblings. Transcriptomic comparisons identified 2279 differentially expressed (DE) genes. Other glossy genes tended to be down-regulated in glossy mutants; by contrast stress-responsive pathways were induced in mutants. Gene co-expression network (GCN) analysis found that glossy genes were clustered, suggestive of co-regulation. Genes that potentially regulate the accumulation of glossy gene transcripts were identified via a pathway level co-expression analysis. Expression data from diverse organs showed that maize glossy genes are generally active in young leaves, silks, and tassels, while largely inactive in seeds and roots. Through reverse genetics, a DE gene homologous to Arabidopsis *CER8* and co-expressed with known glossy genes was confirmed to participate in epicuticular wax accumulation. GCN data-informed forward genetics approach enabled cloning of the *gl14* gene, which encodes a putative membrane-associated protein. Our results deepen understanding of the transcriptional regulation of the genes involved in the accumulation of epicuticular wax, and provide two maize glossy genes and a number of candidate genes for further characterization.

Keywords: cuticular wax, glossy, *Zea mays*, co-expression network, cloning.

INTRODUCTION

The plant cuticle is a hydrophobic layer coating the aerial epidermis for all land plants, and limiting water loss and adverse effects of environmental stresses. The cuticle is composed of the polymer cutin, which serves as the framework of the cuticle, and cuticular waxes, which consist of intracuticular waxes that are embedded in cutin and

epicuticular waxes covering the outmost area of the plant surface (Kunst and Samuels, 2003; Lee and Suh, 2013). Cuticular waxes are composed of a mixture of hydrocarbons, alkanes, aldehydes, primary and secondary alcohols, ketones, and esters, derived from very-long-chain fatty acids (VLCFAs). The precursor VLCFAs are synthesized by

epidermal cells, first in the plastid by joining C₂ acetyl-coenzyme A (acetyl-CoA) into C₁₆ or C₁₈ fatty acids, then transported to the cytoplasm and converted to fatty acyl-CoAs by long-chain acyl-CoA synthetases, and then further elongated into C₂₄ to C₃₄ fatty acids in the endoplasmic reticulum (ER). Cuticular waxes produced in the ER are transported to the plasma membrane (PM), secreted outside cells, and deposited in the epidermis.

Recent studies in Arabidopsis, maize, and other plant species have improved our understanding of the genetic basis of cuticular wax biosynthesis (Bernard and Joubes, 2013). Mutants involved in epicuticular wax accumulation are referred to as eceriferum (*cer*) in Arabidopsis and glossy (*gl*) in maize. Relatively easily scored mutant phenotypes in the two species facilitate cloning of *cer* and *gl* genes. A long-chain acyl-CoA synthetase (LACS), LACS1/CER8, was found to be responsible for the conversion from fatty acid to fatty acyl-CoAs in Arabidopsis (Lu *et al.*, 2009). The CER8 homologs can be identified in maize but functional homologs have not been revealed. The represented genes encoding enzymes involved in four sequential cyclic reactions for fatty acid elongation have been cloned in Arabidopsis, and some were cloned in maize. *CER6* (Fiebig *et al.*, 2000) and *gl4* (Liu *et al.*, 2009a) are ketoacyl synthase (KCS). *KCR1* and *gl8* (*gl8a* and *gl8b*) encode ketoacyl reductase (KCR) (Xu *et al.*, 1997; Dietrich *et al.*, 2005; Beau-doin *et al.*, 2009). Hydroxyacyl dehydrase is represented by PAS2 in Arabidopsis and the counterpart has not been cloned in maize (Bach *et al.*, 2008). CER10 and GI26 are enoyl reductase (Zheng *et al.*, 2005). Elongation beyond C₂₈ is likely to require additional genes *CER2* (Negruk *et al.*, 1996; Xia *et al.*, 1996) and *CER26* (Pascal *et al.*, 2013). The *CER2* homologous gene, *gl2*, has been cloned in maize (Tacke *et al.*, 1995). Before transport from the ER, cuticular waxes are produced from VLCFAs with modifiers such as CER4 (Rowland *et al.*, 2006) and WSD1 (Li *et al.*, 2008) in the alcohol-forming pathway, as well as CER1 (Aarts *et al.*, 1995) and CER3 (Hannoufa *et al.*, 1996) in the alkane-forming pathway. The maize glossy gene *gl1* is a *CER1* homolog and the *gl1* mutant displayed a strong wax-deficient phenotype (Hansen *et al.*, 1997).

The identification of ABC transporters CER5 and WBC11 revealed the mechanism by which waxes are secreted through the PM (Pighin *et al.*, 2004; Bird *et al.*, 2007; McFarlane *et al.*, 2010). The *CER5* homologous gene, *gl13*, was identified in maize that, similarly, functions in the secretion of cuticular waxes (Li *et al.*, 2013). Recent cloning of a novel gene *gl6* that encodes the protein occupying the ER, Golgi, and PM, and wax-like aceroses inclusions were found within epidermal cells, indicative of a Golgi-mediated mechanism of intracellular wax trafficking in which *gl6* is involved (Li *et al.*, 2018).

Beyond wax synthesis and exportation, the cuticular wax synthesis pathway is under transcriptional regulation.

A mutant of *gl15*, an AP2-like transcription factor (TF), causes premature juvenile-to-adult transition and exhibits reduced epicuticular waxes on leaves (Moose and Sisco, 1996). In Arabidopsis, the AP2/EREBP-type TF WIN1/SHN1, as well its homologs SHN2 and SHN3, activate cuticular wax biosynthesis and confer drought tolerance (Aharoni *et al.*, 2004; Broun *et al.*, 2004). Recently, an AP2/ERF TF (a subfamily of AP2/EREBP TF) WRINKLED4 (WRI4) was shown to directly activate genes in the wax biosynthesis pathway (Park *et al.*, 2016). Another AP2/ERF TF DEWAX was identified to be a negative regulator of wax loads in the leaf and stem of Arabidopsis (Go *et al.*, 2014). In addition, cuticular wax accumulation is regulated by multiple MYB TFs, namely MYB30, MYB96, MYB94, and MYB106 (Raffaele *et al.*, 2008; Seo *et al.*, 2011; Oshima *et al.*, 2013; Lee and Suh, 2015; Lee *et al.*, 2016). MYB96 and MYB30 were found to confer resistance to abiotic and biotic stresses, respectively (Raffaele *et al.*, 2008; Lee *et al.*, 2014). The maize MYB gene *gl3* is also responsible for epicuticular wax accumulation (Liu *et al.*, 2012).

To date, at least 30 maize loci that contribute to cuticular wax accumulation have been identified by mutants and a handful of these have been cloned. However, the expression patterns and transcriptional responses upon perturbation of glossy genes have not been systematically investigated. In this study, we compared transcriptomes between mutants and wild-type siblings for each of eight independent glossy genes. A gene co-expression network (GCN) constructed with hundreds of transcriptomic data sets was utilized to understand expression patterns of genes involved in the cuticular wax pathway. With assistance from the GCN, we confirmed that a *CER8* maize homolog is responsible for epicuticular wax biogenesis, and cloned the glossy gene, *gl14*.

RESULTS

Design of RNA-Seq experiments using eight glossy mutants

We compared the transcriptomes of pairs of mutants and their wild-type controls for each of eight glossy genes, including seven cloned genes *gl1*, *gl2*, *gl3*, *gl4*, *gl6*, *gl8*, and *gl26* and one uncloned gene *gl28* (Dietrich, 2002) (Figure 1, Table S1). To minimize the influence of genetic background on transcriptomes, each glossy mutant was first backcrossed into the B73 inbred line for at least six generations. The eight resulting lines were self-pollinated to generate populations, each of which was segregating for a single glossy mutant. Seedlings from each population were phenotypically classified as mutants (glossy phenotype) or wild-types (non-glossy phenotype) (Figure 1a). Within each population, three biological replicates of glossy and non-glossy phenotypes were separately pooled. RNA samples from 48 samples comprising three paired

pools of mutant and wild-type seedlings for each of eight mutants were subjected to paired-end sequencing using the Illumina platform. After removing data for four samples due to poor correlations of read counts per gene with other samples, 44 RNA-Seq data sets remained for subsequent analyses (Table S2). More than 814.5 M pairs of raw reads were obtained, resulting in an average of >18.5 M read pairs per sample. 93.2–97.8% of raw read pairs remained after adaptor and quality trimming (Table S3). Here, 72.9–86.6% of the trimmed reads could be uniquely mapped to the B73 reference genome (B73Ref3) (Table S4) (Schnable *et al.*, 2009).

We have shown previously that RNA sequencing data from pools with phenotypically contrasting individuals can be utilized for gene mapping. This method was referred to as bulked segregant RNA sequencing (BSR-Seq) (Liu *et al.*, 2012). We applied BSR-Seq to genetically map each glossy gene. The mapping locations of the seven cloned genes were concordant with the known genomic locations of

corresponding genes, confirming that correct mutant materials were used and that the categorization of mutants and wild-types was accurate (Figure 1b, Table S1). In addition, the previously uncloned *gl28* was mapped to chromosome 10, consistent with a previous report (Liu *et al.*, 2010).

Identification of differential expression between glossy mutant and wild-type controls

Genes that exhibited differential expression (DE) via comparisons between mutant and wild-type samples were identified for each glossy gene. DE analyses identified 86 to 1017 DE genes from each of eight comparisons, covering 2279 non-redundant DE genes (Tables S5 and S6). Genes related to fatty acid biosynthetic process, abiotic stress response, photosynthesis, integral components of membrane, and cell wall were all over-represented among the DE genes (Figure 2b, Table S7). Specifically, 1376 and 993 genes were up- and down-regulated in mutants in at least one comparison, respectively. Most genes (423/513)

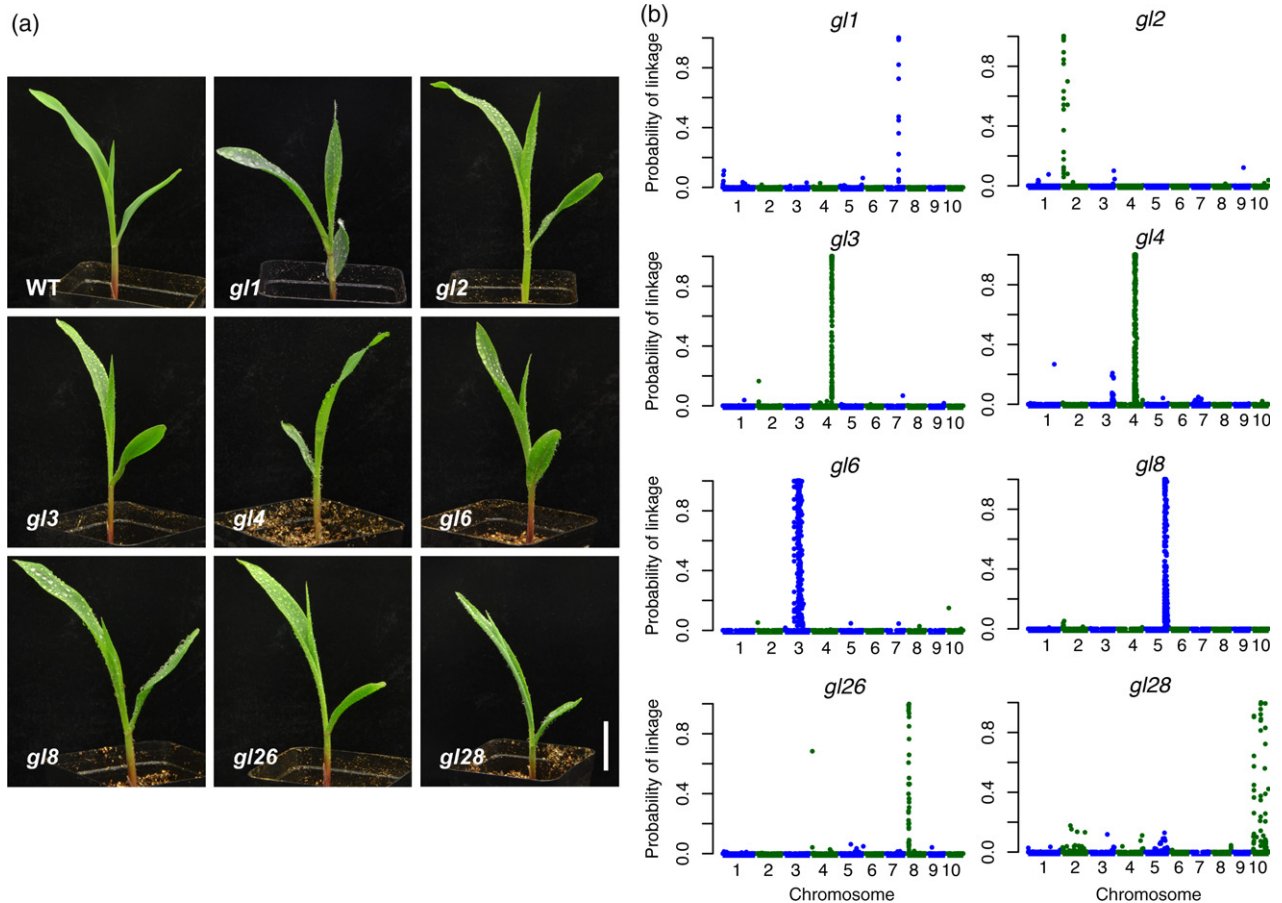


Figure 1. Mapping of each of eight glossy gene via BSR-Seq.

(a) Phenotype of eight glossy mutants and one wild-type control after water spraying.

(b) Mapping of each glossy mutant gene was performed using RNA sequencing of plant pools separately from mutants and wildtypes. The probability of complete linkage of each SNP with the glossy gene was determined by a Bayesian approach and plotted versus the genomic coordinate of the SNP. The cloned genes, *gl1*, *gl2*, *gl3*, *gl4*, *gl6*, *gl8*, *gl26*, were mapped to the expected locations. The uncloned gene, *gl28*, was mapped to chromosome 10.

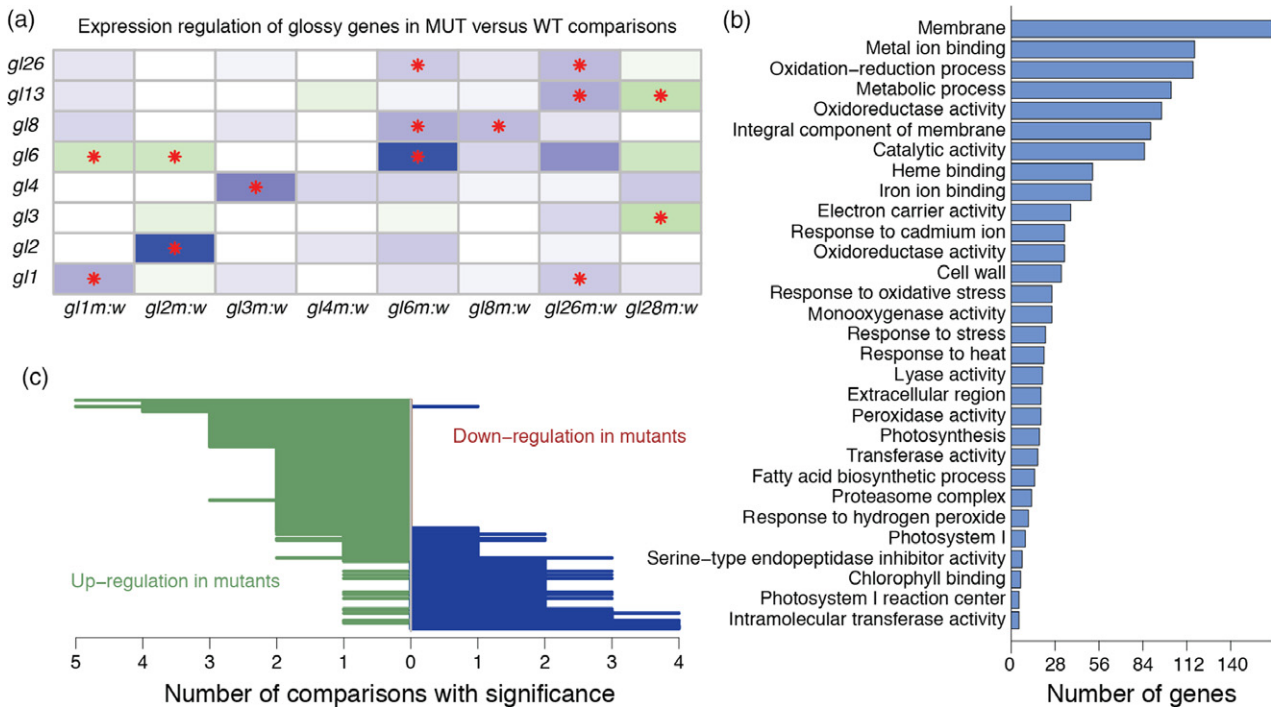


Figure 2. Differential expression between mutants and wildtypes of eight glossy genes.

(a) Expression regulation of eight cloned genes, indicated by \log_2 fold change of gene expression in mutants versus wildtypes, were color-coded. Blue designates down-regulation in mutants relative to wild type, while green designates up-regulation. The color intensity represents the level of fold change. Saturated intensity is set at eight-fold changes (\log_2 fold changes are -3 or 3). A red asterisk indicates the significance of a given gene from a differential expression (DE) test.

(b) Significant gene ontology (GO) terms ($q < 0.05$) from the GO enrichment test were listed.

(c) Here, 513 genes showed DEs for at least twice out of eight comparisons of glossy mutants versus wild-types. For each gene, the level of up-regulation (green) or down-regulation (blue) in the mutants was determined and plotted. From top to bottom, the number of differences between up- and down-regulation was used to facilitate sorting.

that were significantly DE in more than one comparison were only either up- or down-regulated (Figure 2c). Gene ontology (GO) enrichment tests were performed on 301 and 164 genes that were up- and down-regulated in mutants in at least two comparisons, respectively. Genes related to fatty acid biosynthetic were highly enriched among down-regulated genes, while genes responding to stress, particularly abiotic stress, were highly enriched among up-regulated genes (Figures S1 and S2). These results indicated that the expression of fatty acid biosynthetic genes generally tend to be down-regulated in glossy mutants versus their wild-type controls, and stress-defensive responses were induced in the mutant plants, perhaps as a consequence of stresses imposed by reductions in epicuticular wax loads.

We examined expression regulation of known glossy genes, including *gl13*, another cloned glossy gene putatively encoding an ABC transporter (Li *et al.*, 2013) (Figure 2a). All known cloned glossy genes exhibited significant DE in at least one mutant versus wild-type comparison. Five glossy genes exhibited DE in at least two such comparisons. The *gl1*, *gl2*, *gl6*, *gl8*, and *gl26* genes were down-regulated in their respective mutants as compared with wild-type controls. The *gl3* gene, which

encodes a MYB transcription factor was up-regulated in *gl28* mutants as compared with wild-type controls, suggestive of feedback regulation. By contrast with all other examined glossy genes, *gl2* only exhibited DE in the *gl2* mutants and wild-types comparison.

Construction of a GCN

To understand expression patterns of glossy genes in diverse tissues/stages and under different environmental conditions, we retrieved 324 B73 RNA-Seq data sets from the Sequence Read Archive (SRA) and constructed a GCN using normalized read counts per gene. The resulting GCN consists of 13 211 genes in 34 modules (Figure 3a, Table S8). Of the eight cloned glossy genes, seven were in the B73 GCN and all were clustered in a single module (the turquoise module) that contained 1774 genes, suggesting that glossy genes are transcriptionally co-regulated (Table S8). Within the turquoise module, for each gene, the Mean of Absolute Correlation with glossy genes (MAC) was determined (Experimental procedures). MAC values of genes in the turquoise module, which indicate their similarity in expression to genes in the cuticular wax synthesis pathway, ranged from 0.18 to 0.85 (Table S9). Note that MAC values of glossy genes per se were also determined.

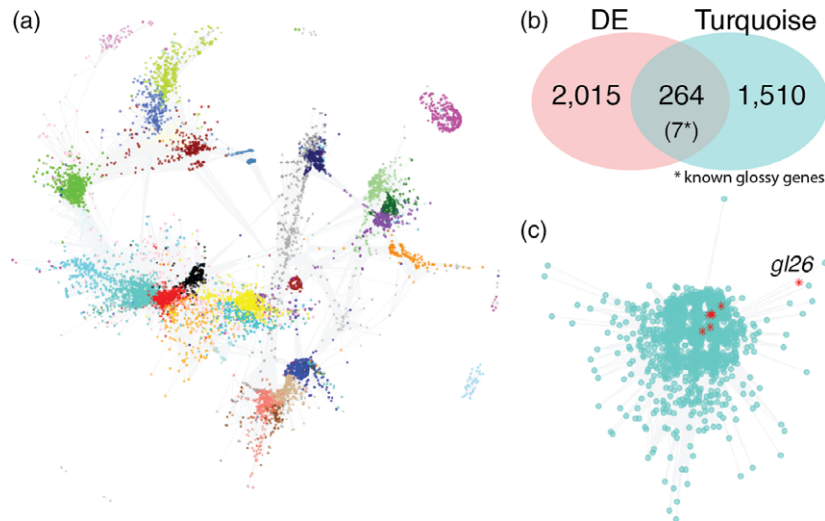


Figure 3. Gene co-expression analysis of glossy genes.

(a) Publicly available RNA sequencing data from various B73 samples were processed to determine gene expression. In total, 13 211 genes were added to the constructed gene co-expression network (GCN), which contained 34 modules, represented by colors. (b) Visualization of the partial turquoise network, known glossy genes are highlighted in red. (c) Venn diagram of genes with differential expression (DE) at least in one comparison between glossy mutants versus wildtype, and genes in the turquoise module from B73 GCN. In total, seven known glossy genes (*gl1*, *gl2*, *gl3*, *gl4*, *gl6*, *gl13*, *gl26*) in the GCN all shown to be DE were present in the turquoise module. Note that *gl2* only showed DE in the *gl2* mutant analysis and compared with wild-type controls.

Most glossy genes exhibited high MAC values, from 0.53 to 0.81 and with the average MAC value of 0.73, indicative of a tight connection among glossy genes (Figure 3b). Of genes in the turquoise module, 264 were DE in at least one comparison between glossy mutants and wild-types. DE genes from the turquoise module contained all seven glossy genes, of which 6 out of 7 were DE in at least one comparison of other glossy genes (Figure 3c). The average of MAC values of 257 DE genes in the turquoise module, with the exclusion of seven glossy genes, is higher than that of the rest of genes in the module (*t*-test, $P = 0.04$), indicating that, overall, expression patterns of DE genes in the turquoise module are more similar to glossy genes. GO enrichment analysis indicated that genes in the wax biosynthesis and photosynthesis pathways were overrepresented among the DE genes in the turquoise module (Table S10). Glossy genes and photosynthesis-related genes were typically expressed at higher levels in young or newly emerged leaves across vegetative stages, leaf bases, silks, meiotic tassels, and anthers, but at lower levels in roots and seeds, particularly seed endosperms (Figure S3). Taken together, the turquoise module contains the genes co-expressed with known glossy genes that are enriched in the 264 DE genes of this module. We therefore hypothesized that it includes previously uncloned glossy genes involved in the accumulation of cuticular wax.

Co-expression of glossy genes is likely to be regulated by common transcription factors (TFs). To identify potential regulators, we employed a method called Pathway-level co-expression (PLC) analysis to identify TFs

co-expressed with multiple glossy genes (Wei *et al.*, 2006; Chun and Keles, 2010). As a result, 69 co-expressed TFs were found with at least three of six cloned genes *gl1*, *gl2*, *gl4*, *gl6*, *gl8*, and *gl26* (Table S11). Two genes showing co-expression with all six cloned genes are both MYB genes, AC197146.3_FG002 and GRMZM2G162434 (*gl3*) (Liu *et al.*, 2012), both of which are in 264 turquoise-DE genes. The identification of *gl3* via this process indicated that the PLC analysis algorithm successfully captured genes that regulated wax synthesis. In addition, a homolog of Arabidopsis *WIN1*, GRMZM2G085678, displayed co-expression with five glossy genes. Of 35 genes showing a co-expression connection to at least four glossy genes, MYB genes ($N = 10$) were over-represented ($\chi^2 = 9.3$, $df = 1$, $P = 0.002$). In Arabidopsis, some MYB genes are activators or suppressors of wax synthesis (Raffaele *et al.*, 2008; Seo *et al.*, 2011; Go *et al.*, 2014; Lee and Suh, 2015). Our results indicate that multiple MYB TFs also appear to regulate wax synthesis in maize.

A CER8 homolog from turquoise-DE genes

The 264 turquoise-DE genes contain a gene, GRMZM2G101875, that exhibited a high MAC value of 0.75 and was homologous to Arabidopsis CER8 (Lu *et al.*, 2009), which is involved in the conversion of fatty acids to fatty acyl-CoAs for biosynthesis of cuticular waxes in the ER. An ethyl methanesulfonate (EMS) mutant, *ems12581*, carrying a G/A mutation at the splicing donor site of the 12th intron of GRMZM2G101875 was identified from the Maize EMS induced Mutant Database (MEMD) (Figure 4a)

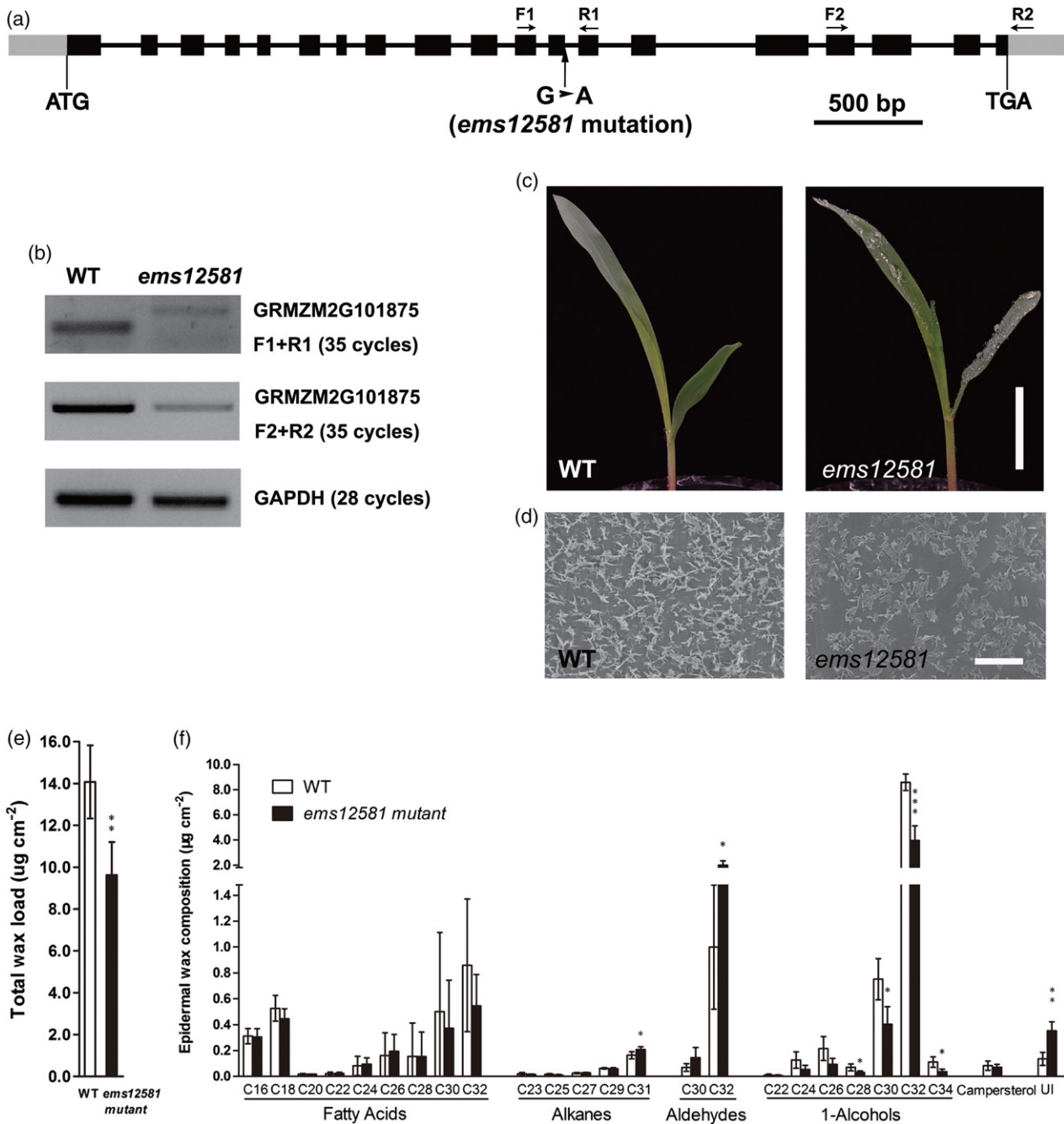


Figure 4. GRMZM2G101875 mutant.

(a) Gene structure of GRMZM2G101875 and transcriptional start, end, point mutation of the *ems12581* mutant, and primers positions were labeled. Black boxes represent exons, grey boxes represent untranslated region and lines represent introns. Approximate positions and orientation of primers used for semi-RT-PCR, F1 and R1, F2 and R2, are indicated as arrows.

(b) Semi-RT-PCR was used to detect the gene expression of GRMZM2G101875 between wildtype (WT) and *ems12581* mutants in seedlings by primers indicated in (a), and GAPDH was used as a control.

(c, d) Mutant and wild-type photographs from water spraying and SEM (BAR = 3 cm). Leaf epicuticular wax accumulation in wild-type and *ems12581* seedlings detected via SEM ($\times 10\ 000$ magnification, bar = 3 µm).

(e, f) Total epicuticular wax loads and wax components of mutants and wildtypes. Values are means of four biological replicates ± SD. UI represents unidentified components and asterisks indicate statistically significant differences between wild-type controls and *ems12581* mutants (* $P < 0.05$, ** $P < 0.01$, Student's *t*-test).

(Lu *et al.*, 2018). Segregation analysis of 16 individuals showed that glossy phenotypes perfectly matched phenotypic expectation from genotyping data of the G/A

mutation site (Table S12). The mutation caused a reduced accumulation of transcripts and the accumulation of intron retention transcripts containing 12th intron (Figure 4b).

The mutant seedlings displayed a typical glossy phenotype, indicative of decreased accumulation of epicuticular waxes (Figure 4c). Examination of wax accumulation on leaf surfaces via scanning electron microscopy (SEM) showed that fewer wax crystals were deposited on the surfaces of *ems12581* mutant leaves as compared with wild-type leaves (Figure 4d). Total wax loads and composition of *ems12581* mutants were further quantified by GC–mass spectrometry. Relative to wildtypes, total leaf surface wax on *ems12581* mutants was reduced by 32%, from $14.1 \mu\text{g cm}^{-2}$ in wildtypes to $9.6 \mu\text{g cm}^{-2}$ (Figure 4e). Altered wax components were also observed in mutants versus wildtypes, namely, decreased amounts of C_{28} , C_{30} , C_{32} , C_{34} primary alcohols but increased amounts of C_{32} aldehydes and C_{31} alkanes in *ems12581* mutants (Figure 4f). The results supported the conclusion that the CER8 homolog GRMZM2G101875, termed ZmCER8, participates in accumulation of epicuticular waxes in maize, demonstrating that the discovery of unknown glossy genes can be facilitated with GCN data.

Cloning of *gl14*

We further used GCN information to assist with the cloning of *gl14*, which exhibits a classical glossy phenotype (Figure 5a). The *gl14* gene has been mapped to chromosome 2 (Sprague, 1990; Schnable *et al.*, 1994). Three additional *gl14* mutants (*gl14-EMS-94-1001-3651*, *gl14-EMS-94-1001-3307*, and *gl14-EMS-AEW-A632-44*) were generated through EMS mutagenesis of the inbred line A632 and confirmed to be allelic to *gl14-ref*. Each allele was backcrossed to A632. For each mutant allele, an F_2 segregating population was developed, and F_2 mutant and wild-type siblings were separately pooled for BSR-Seq mapping (Table S13). All three alleles were mapped to chromosome 2 using 44 410 to 52 519 SNPs for BSR-Seq comparisons, and the strong mapping peaks around the interval between 63.0 and 126.3 Mb were observed in the mapping results for the *gl14-EMS-94-1001-3307* and *gl14-EMS-AEW-A632-44* alleles (Figure 5b, Figure S4). Broad mapping intervals are probably a consequence of the fact that the *gl14* gene is located near the centromere (*c.* 94 Mb) where recombination is highly suppressed (Liu *et al.*, 2009b).

Assessment of functional impacts of nucleotide polymorphisms identified using RNA-Seq of all three EMS-induced mutants, through the software SNPEff (Cingolani *et al.*, 2012), found 3659 high-impact variants, such as mutations at splice acceptor/donor sites, losses of translational start sites, or gains of translational stop site, in 3605 genes, among which 38 were located in the mapping interval. Of 38 genes, three overlapped with genes in the GCN turquoise module (Figure 5b). These three genes exhibited moderately high MAC values, ranging from 0.43 to 0.63. One of these genes, GRMZM5G806387, carried G/C to A/T changes that were characteristic of EMS-type mutations.

All three mutant alleles contained such a mutation, resulting in a premature stop codon in each mutant allele. Two of these alleles, *gl14-EMS-94-1001-3307* and *gl14-EMS-94-1001-3651*, harbored the same mutation at position 89 243 661, and the allele of *gl14-EMS-AEW-A632-44* had a mutation at position 89 243 516 (Figure 5c). All three EMS-type mutations inferred from RNA-Seq data were confirmed by Sanger sequencing using DNAs from independent mutant plants (Figure S5). Sanger sequencing of the coding sequence of the *gl14-ref* allele identified a point mutation (C to T) causing an amino acid (aa) change from arginine (R) to cysteine (C) at the 47th aa (R47C) of the G114 protein (Figure S6). The *gl14* gene contains a single exon, encoding a 160-aa protein. The mutation in the reference allele is located at the conserved MARVEL domain (DUF588) containing three transmembrane helices (Sanchez-Pulido *et al.*, 2002), and arginine at the 47th aa is highly conserved across plant species (Figure S7). SEM showed decreased wax crystals on the leaf surface of *gl14-EMS-94-1001-3651* mutants as compared with wild-type seedlings (Figure 5a). Consistently, total leaf surface waxes on *gl14* mutants were reduced by 33%, from $11.9 \mu\text{g cm}^{-2}$ in wild-type seedlings to $7.9 \mu\text{g cm}^{-2}$ (Figure 5d). Wax composition analysis showed reduced amounts of C_{28} , C_{30} , C_{32} , C_{34} primary alcohols, and C_{32} fatty acids, but elevated amounts of C_{32} aldehydes and C_{31} alkanes on *gl14* mutant leaves (Figure 5e). Our result provided strong evidence that GRMZM5G806387 is the *gl14* gene that presumably encodes a membrane-associated protein.

DISCUSSION

In this study, we compared leaf transcriptomes of glossy mutants with those of their wild-type siblings and examined transcriptomic regulation of glossy genes. We found that glossy genes are co-regulated, a characteristic that can be used to identify unknown glossy genes. Two maize glossy genes identified in this manner demonstrate the value of our approach, thereby defining a strategy to facilitate the discovery of causal genes underlying traits of interest.

Revelation of expression patterns of maize glossy genes

We attempted to understand expression patterns of maize glossy genes responsible for epicuticular wax accumulation, and transcriptomic responses upon perturbation of glossy genes. Dysfunction of most glossy genes resulted in the down-regulated expression of other glossy genes, suggesting that the entire wax pathway may be inactivated in most glossy mutants. At the same time, pathways responsive to stresses were induced in glossy mutants. Stresses are likely to be imposed by elevated non-stomata water losses owing to reduced wax loads on leaf surfaces (Li *et al.*, 2013, 2018). Stress responses are also possibly signaled by changed accumulation of VLCFAs on leaves, supported by the findings that genes involved in wax

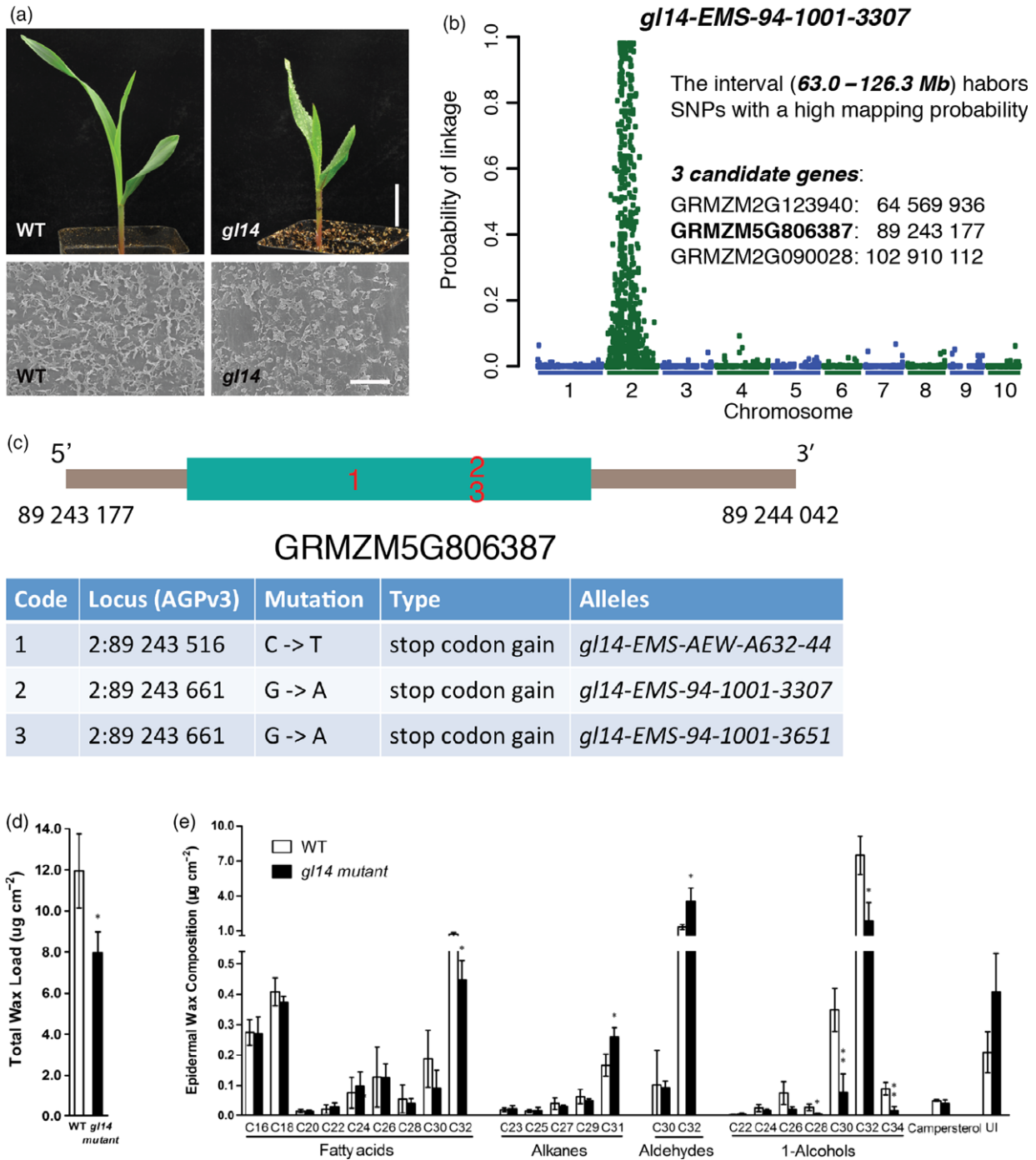


Figure 5. *gl14* cloning.

(a) Phenotype of the *gl14* mutant (the *gl14-EMS-94-1001-3307* homozygous mutant) and wildtype after water spraying (bar = 3 cm) and SEM photographs ($\times 10\,000$ magnification, bar = 3 μm).

(b) BSR-Seq to map the *gl14* gene using the mutant allele of *gl14-EMS-94-1001-3307*. The mapping interval was based on SNPs showing a high probability (>0.975) of complete linkage between the SNP and the *gl14* gene. Candidate genes are the genes harboring at least one large-effect variant in EMS mutants and in the turquoise co-expression module.

(c) The candidate gene, GRMZM5G806387, was confirmed to be the *gl14* gene by showing that three alleles from at least two independent EMS mutagenesis events carried EMS-type mutations, all of which introduce premature stop codons, and presumably caused the encoded truncated proteins.

(d, e). Total epicuticular wax loads, wax component analysis and comparison in *gl14* mutants (the *gl14-EMS-94-1001-3307* homozygous mutant) and wildtype. Values are means of three biological replicates \pm SD. UI indicates unidentified and asterisks indicate statistically significant differences between wildtype and *gl14* mutants (* $P < 0.05$, ** $P < 0.01$, Student's *t*-test).

biosynthesis participate in both biotic and abiotic stress responses (Aharoni *et al.*, 2004; Raffaele *et al.*, 2008; Seo *et al.*, 2011; De Bigault Du Granrut and Cacas, 2016).

Activation of most glossy genes in young leaves, silks, meiotic tassels, and anthers are consistent with the hypothesis that wax components are critical for the development and/or functions of these organs. Conceivably, active cell development at young leaf stages and flowering requires the maintenance of a high moisture environment. Increased production of cuticular waxes protects organs from non-stomatal water losses, which may incrementally contribute to preserve necessary moisture in these organs. In Arabidopsis, *WIN1/SHN1* is highly expressed during flowering time, presumably activating wax biosynthesis (Broun *et al.*, 2004). Overexpression of *WIN1/SHN1* confers drought tolerance. However, organ non-specific and constitutive *WIN1/SHN1* expression has pleiotropic alterations in growth and development (Aharoni *et al.*, 2004). To breed enhanced drought tolerance crops through modifying wax loads, it would be highly valuable to identify TFs that can specifically tune wax expression on those organs that would benefit from high cuticular wax loads.

Candidate transcriptional regulators of wax accumulation

Epicuticular waxes are spatially and temporally expressed and our GCN data indicated that expression of glossy genes is strictly regulated. We employed PLC analysis to identify 69 TFs whose expression is highly correlated with the expression of glossy genes. Among these TFs, MYB TFs are over-represented. Multiple MYB TFs, namely, MYB30, MYB96, MYB94, and MYB106, have been demonstrated to regulate cuticular wax biosynthesis in Arabidopsis (Raffaele *et al.*, 2008; Seo *et al.*, 2011; Oshima *et al.*, 2013; Lee and Suh, 2015; Lee *et al.*, 2016). Different MYB TFs may share targeted genes in wax biosynthesis, and/or regulate distinct targets. Experimental data from Arabidopsis showed that MYB30 and MYB96 directly activated genes synthesizing VLCFAs, while MYB94 regulated diverse genes including some involved in producing VLCFAs, as well as genes participating in VLCFA modification such as *CER1* in the alkane-forming pathway and *WSD1* in the alcohol-forming pathway (Raffaele *et al.*, 2008; Seo *et al.*, 2011; Lee and Suh, 2015). MYB106 promotes wax biosynthesis by targeting *WIN1* (Broun *et al.*, 2004). In maize, only one MYB gene, *g13*, has been confirmed to be responsible for wax biosynthesis. From expression data of diverse tissues, *g13* expression was only observed in a handful of tissues such as young leaves, meiotic tassels, and silks, in which almost all known glossy genes were expressed at relatively high levels (Figure S8). However, expression of some glossy genes was detected beyond those tissues, indicating that *g13*-independent activation exists. In roots, some MYB TFs were silenced, including *g13*, but others, including GRMZM2G044824 (*MYB9*), GRMZM2G104789 (*MYB36*), GRMZM2G017268 (*MYB93*),

and GRMZM2G110135 (*MYB93*) were induced. The MYB genes induced might specifically regulate a subset of glossy genes in roots (Figure S9), which possibly involves the accumulation of long chain fatty acids required for producing suberin (Graca, 2015).

In addition to MYB TFs, AP2/EREBP TFs are also important transcriptional regulators for wax production. Overexpression of either of *WIN1/SHN1* and its homologs, *SHN2* and *SHN3*, changed surface structure and composition in Arabidopsis, including reduced stomatal density and elevated production of cuticular waxes, and affected epidermal cell differentiation. Altering cell fate is reminiscent of the function of *g15* in maize. The loss of *g15* function induces early juvenile-to-adult phase transition of epidermal cells, which results in alterations in wax loads. *WRI4* and *DEWAX* are two AP2/ERF TFs that directly positively and negatively regulate genes in the wax pathway, respectively. Our Sparse Partial Least Squares (SPLS)-based pathway-level co-expression analysis also identified three AP2/EREBP TFs GRMZM2G085678, GRMZM2G141219, and GRMZM2G457562. Among these, GRMZM2G085678 is a homolog of Arabidopsis *WIN1/SHN1*. Based on gene expression in diverse tissues from different stages, all three AP2/EREBP maize genes are transcriptionally positively correlated with glossy genes, indicating that they are not negative regulators as *DEWAX* is still functional (Figure S9). In addition to MYB and AP2/EREBP TFs, other gene families whose expression is correlated with glossy genes include other TF families such as bHLH-TFs and mitochondrial transcription termination factor family proteins. With the established transformation technology, developed reverse genetic resources (Settles *et al.*, 2007; Lu *et al.*, 2018) and advances in genome editing technologies (Gao, 2018), the TF candidates that potentially regulate wax production are ready for experimental examination.

Two maize glossy genes

Gene co-expression network analysis aided the identification of two maize glossy genes, GRMZM2G101875 (*ZmCER8*), an Arabidopsis *CER8* homolog, and *G114*, a glossy gene with unknown function. In Arabidopsis, *LACS1/CER8* is postulated to be a direct VLCFA modifier due to the altered composition of VLCFA derivatives in *cer8* mutants (Jenks *et al.*, 1995). We found increased amounts of C₃₂ aldehydes and C₃₁ alkanes, and decreased amounts of C₂₈, C₃₀, C₃₂, C₃₄ primary alcohols in *ems12581* mutants. Consistent with Arabidopsis *cer8* mutants, changes were largely observed on very-long-chain (C₂₈ and longer chain) derivatives, although alkanes derivatives are a major group that is reduced in Arabidopsis *cer8* mutants. Our data therefore support the hypothesis that *CER8/LACS1* primarily functions in the conversion of VLCFAs to fatty acyl-CoAs from which cuticular waxes are derived (Lu *et al.*, 2009). It is likely that the lack of fatty

acyl-CoAs as precursors has a complicated effect on the production of VLCFA derivatives, and the effects appear to be different between Arabidopsis and maize.

The *gl14* gene carries a conserved MARVEL domain (DUF588) containing three transmembrane helices. The mutation in the *gl14-ref* mutant allele is located at a highly conserved amino acid in the MARVEL domain, which is expected to influence membrane-related function. Given the weakly expressed glossy phenotype of *gl14-ref* mutants (Dietrich, 2002) and the strong glossy phenotype of the EMS mutant, which presumably produces a truncated protein (Figure S10), *gl14-ref* is likely to represent a leaky allele. This result also suggests that the effect of G114 on cuticular wax production is not marginal.

In summary, our transcriptomic study revealed expression relationships among glossy genes, genes in other pathways, and transcriptional regulators. GCN and transcriptomic responses to perturbation of glossy genes provide a unique guide for prioritizing candidate genes for identifying unknown glossy genes. These findings could help to accelerate discovery of unknown glossy genes and provide useful information for a possible rewiring of cuticular wax biosynthesis that has the potential to improve important agricultural traits such as enhanced drought tolerance or pathogen resistance.

EXPERIMENTAL PROCEDURES

Genetic materials

The reference alleles of each of genes (*gl1*, *gl2*, *gl3*, *gl4*, *gl6*, *gl8*, *gl26*, *gl28*) were introduced to the inbred line B73 via at least six backcrosses. Self pollinations of heterozygous individuals from this backcrossing program were used to generate families segregating for specific reference alleles. Our ability to discriminate mutants and wild-type siblings in these families was enhanced by spraying water on seedlings at the two or three leaf stage. Seedlings whose leaves were covered by small water droplets were classified as mutants. Seedlings without the water-droplet phenotype were categorized as wild-type. Rare seedlings with ambiguous phenotypes were not used for further analyses.

The EMS mutant of GRMZM2G101875, *ems12581*, was ordered from the Maize EMS induced Mutant Database (MEMD) (<http://111.203.21.178/memd>) (Lu *et al.*, 2018).

The reference allele (*gl14-ref*) was described by Sprague (Sprague, 1990) and ordered from the Maize Genetics COOP Stock Center. Three additional mutant alleles of *gl14* were generated previously via ethyl methanesulfonate (EMS) mutagenesis of the inbred line A632 (Dietrich, 2002).

RNA extraction and sequencing

For all RNA-Seq experiments, mutants and sibling wild-type controls from a single segregating family generated as described above were separately pooled. Pooled tissues were subjected to total RNA extraction (RNeasy mini kit; Qiagen, <https://www.qiagen.com/>) followed by treatment with DNase I. Total RNA samples were quality checked and used to prepare sequencing libraries. With the exception of the *gl2*-related samples, all samples were

sequenced as 2× 101-bp paired ends in an Illumina HiSeq2000 instrument at Macrogen Inc. in Korea (<https://www.illumina.com/>). The *gl2* RNA-Seq experiment was performed using 2× 150-bp paired-end sequencing in an Illumina HiSeqX instrument at Novogene, China. Three biological replicates per experiment of the glossy gene were performed. To reduce technical variation during sequencing, all six samples associated with a given *glossy* gene were sequenced in the same lane.

Read trimming, alignment, and read counts per gene

Raw reads were trimmed to remove adaptor contamination and low-quality base pairs with Trimmomatic (v3.6) software (Bolger *et al.*, 2014). The minimal requirement of read lengths was 50 bp. Clean reads were aligned to the B73 reference genome (B73Ref3) with the RNA-Seq aligner, STAR (STAR_2.5.2a_modified) (Dobin *et al.*, 2013). A qualified alignment requires at least a 50-bp match, at least 98% of the length of a read aligned to the reference sequence, and at most two mismatches. Only uniquely mapped reads were used for subsequent analyses. Read counts per gene were determined using STAR.

Discovery of variants

GATK (v3.3) used alignments to discover SNPs using all RNA-Seq data, and to determine read depths per allele for each sample (McKenna *et al.*, 2010). Before GATK SNP calling, STAR alignments in the BAM format were modified with read groups added using the module AddOrReplaceReadGroups (v2.6.0-SNAPSHOT) in the Picard package (<https://github.com/broadinstitute/picard>). Only bi-allelic SNP sites were retained.

BSR-Seq mapping

Genomic locations of glossy genes were determined via BSR-Seq (Liu *et al.*, 2012).

Analysis of differential expression

DESeq2 (1.14.1) was used to identify differentially expressed genes (Love *et al.*, 2014). The parameter 'independent Filtering' was turned on to remove genes that were unlikely to be differentially expressed statistically. Multiple testing correction was accounted for using a 10% false discovery rate (FDR) (Benjamini and Hochberg, 1995).

Gene ontology analysis

Gene ontology terms that were over-represented in a set of genes were identified using the random resampling method ($N = 10\,000$) in the GOSec enrichment test (Young *et al.*, 2010). GO terms with adjusted *p*-values less than 0.05 were considered to be over-represented terms (Benjamini and Hochberg, 1995). The online tool AgriGO (bioinfo.cau.edu.cn/agriGO) (Tian *et al.*, 2017) was used to visualize GO networks. Fisher's exact test was used in AgriGO GO enrichment tests and the Yekutieli method was implemented to account for multiple tests under dependency (Benjamini and Yekutieli, 2001).

Construction of the GCN

B73 RNA-Seq data were downloaded from the NCBI sequence read archive (SRA) (Table S14), which were generated from multiple tissues including but are not limited to seedlings, leaves, crown roots, tap roots, whole roots, shoots, seeds, steles, stems, pollen, ears, and tassels. Raw reads were trimmed to remove adaptors and low-quality base pairs via Trimmomatic

(v3.3). Clean reads were aligned to the B73Ref3 with STAR, followed by the generation of normalized FPKM (fragments per kb of transcript per million reads) using cufflinks (v2.1.1) software (Trapnell *et al.*, 2010). The normalized data were used to construct the GCN with the WGCNA R package (Langfelder and Horvath, 2008).

Determination of the mean of absolute correlation with glossy genes (MAC)

Normalized read counts per gene of all RNA-Seq data sets used for GCN analysis were used for calculating the Pearson correlation of each gene from the turquoise module with each of glossy genes in the module. The mean of absolute values of correlation with multiple glossy genes, referred to as MAC, was used to indicate the similarity in expression of a gene to genes in the cuticular wax synthesis pathway. When calculating the MAC of a glossy gene, the correlation with itself was excluded from the calculation of a MAC value.

Identification of transcription factors regulating glossy genes

Sparse Partial Least Squares regression (Chun and Keles, 2010), which has demonstrated to be effective in identifying functionally associated regulatory relationships with multi-dimensional biological data, was used to associate six known glossy genes with annotated TFs. Six glossy genes including *gl1*, *gl2*, *gl4*, *gl6*, *gl8*, *gl26* as well as 2604 maize TFs downloaded from PlantTFDB (Jin *et al.*, 2017) were used in the SPLS analysis. The expression data of six glossy genes and all 2604 TFs were extracted from the 324 RNA-seq data sets used in GCN analysis. SPLS analysis was performed using an R package called 'splsp' from the CRAN library (<https://CRAN.R-project.org/package=splsp>). All TFs that had a significant partial correlation with a glossy gene were taken into account toward the calculation of their frequencies of correlation with six pathway genes. Pathway-level co-expression (PLC) analysis, as illustrated earlier (Wei *et al.*, 2006), was finally performed to summarize and rank all TFs based on the number of glossy genes with which they were partially correlated. The TFs that were partially correlated with high number of wax pathway genes were considered to be the potential pathway regulators.

Generation of heatmaps using RNA-Seq expression data

The transformed gene expression values with log₂ (FPKM+0.1) were then standardized with Z-score method for clustering analysis. Standardized scores with original FPKM less than 0.1 were converted to the lowest standardized value across all data points. Hierarchical clustering analysis and heatmaps were performed with the R package pheatmap (<https://CRAN.R-project.org/package=pheatmap>) using Pearson's correlation.

Scanning electron microscopy

Second-leaf samples were fixed on the spindle and frozen in liquid nitrogen, and dried in a vacuum-drying oven for SEM analysis (SU8010; HITACHI, Japan, <http://www.hitachi.com/>) (Aharoni *et al.*, 2004).

Analysis of wax composition

Wax extraction and gas chromatography (GC)-mass spectrometry (MS) analysis were performed according to the described methods with some modifications (Chen *et al.*, 2011). Mutants and wild-types were grown in the substrate of roseite and sands (1:1) at growth chamber (25°C) under 16/8 h light/dark. Second leaves

from three-leaf plants containing 5–6 g dry matter were collected and instantly immersed in 1000 µL chloroform for 45 sec, the extracts containing 10 mg of tetracosane (Fluka) as an internal standard were transferred into opened reactive vials, dried with nitrogen gas (Pressure Blowing Concentrator; N-EVAP), and derivatized by adding 20 µL of *N,N*-bis-trimethylsilyltrifluoroacetamide (Macherey-Nagel) and 20 µL of pyridine and incubated for 40 min at 70°C. These derivatized samples were then analyzed by GC-FID (Agilent, Technologies) and GC-MS (Agilent gas chromatograph coupled to an Agilent 5973N quadrupole mass selective detector, <https://www.agilent.com/>).

Reverse transcription PCR

For GRMZM2G101875 expression analysis, samples of young leaves at 12 days after sowing were collected, and then were used to extract total RNAs using TRIzol reagent (Invitrogen, <https://www.thermofisher.com/>). RT-PCR analysis was conducted with primers F1 and R1, F2 and R2. Primer sequences, F1, 5'-GCTGAAGCCGACTCTACTGG-3'; R1, 5'-GCTTTCATGCTTGCCAGTTT-3'; F2, 5'-TTGGAGAGATGACCCAGAC-3'; R2, 5'-CGGCCTCACTCTTCTCAAC-3'. Maize *GAPDH* was used as the internal control. *GAPDH*-F, 5'-AGGATATCAAGAAAGCTATTAAGGC-3', *GAPDH*-R, 5'-GTAGCCCCACTCGTTGTCG-3'.

Analysis of functional effects of variants of *gl14* EMS mutants

GATK variant VCF outputs were used to annotate variants with SnpEff (4.3r) (Cingolani *et al.*, 2012). The prioritized candidates of causal *gl14* EMS mutations are variants that are located in the mapping interval, G to A or C to T transitions, and annotated as high-impact variants.

Sanger sequencing validation of EMS-induced *gl14* mutations

PCR amplicons from EMS mutants with primers designed on EMS mutation sites were purified and Sanger sequenced. Primers *gl14_320F*, 5'-CGTCATGCTCCGTAACCAG-3'; *gl14_497R*, 5'-GAG-GAAGACGAGCCAGGAG-3' were used to sequence the mutation of the *gl14-EMS-AEW-A632-44* allele. Primers *gl14_417F*, 5'-GCTGCCTACTCGCTGGTATC-3'; *gl14_623R*, 5'-CGTGATGTTGGCA GAAAAG-3' were used to sequence mutations of *gl14-EMS-94-1001-3651* and *gl14-EMS-94-1001-3307* alleles.

Sanger sequencing to identify nucleotide polymorphisms in the *gl14-ref* allele

Primers designed to amplify sequences covering the whole coding sequence were used to sequence the *gl14-ref* allele: *gl14-F*, 5'-CCTCCCCATAAATGCACTGT-3'; *gl14-R*, 5'-AACGCATAAGCTGCCA-TACA-3'.

ACCESSION NUMBERS

RNA-Seq data for eight glossy comparisons were deposited at Sequence Read Archive (SRA) under accession number SRP155608. RNA-Seq of three *gl14* EMS mutants and their wild-type controls were deposited under accession number SRP155600.

ACKNOWLEDGEMENTS

We thank Drs. Jianxin Shi and Guorun Qu, and Ms. Qian Luo (Shanghai Jiao Tong University) for assistance with the GC-FID

and GC-MS data collection and data analyses. We thank Ms. Lisa Coffey (Iowa State University) for creating and maintaining the B73 backcross stocks carrying the *gl* mutants. Mr Dan Bade (Iowa State University) conducted PCR and sequencing experiments of *glossy* loci. This work was supported in part by the National Key Research and Development Program of China (grant no. 2016YFD0101002), the National Natural Science Foundation of China (grant no. 31330056) and the Agricultural Science and Technology Innovation Program of CAAS. This is contribution number 19-020-J from the Kansas Agricultural Experiment Station.

CONFLICT OF INTEREST

The authors declare no conflict of interest.

SUPPORTING INFORMATION

Additional Supporting Information may be found in the online version of this article.

Figure S1. Network visualization of GOs related to the wax biosynthesis pathway.

Figure S2. Network visualization of GOs related to the abiotic stress pathway.

Figure S3. Heatmap of expression of *glossy* genes and genes involved in photosynthesis.

Figure S4. BSR-Seq mapping result using the *gl14*-EMS-AEW-A632-44 mutant allele.

Figure S5. Validation of *gl14* mutations via Sanger sequencing.

Figure S6. Sequence comparison between the *gl14*-ref and the B73 allele.

Figure S7. Alignments of protein sequences of a partial MARVEL region.

Figure S8. Heatmap of expression of *glossy* genes.

Figure S9. Heatmap of expression of *glossy* genes and 35 top TFs from ICE analysis.

Figure S10. Seedling phenotypes of different *gl14* alleles after water spraying.

Table S1. List of *glossy* genes examined.

Table S2. List of RNA-Seq samples.

Table S3. Trimming summary of RNA-Seq data of eight *glossy* mutants.

Table S4. Alignment summary of RNA-Seq of eight *glossy* mutants.

Table S5. Summary of DE between mutants and wildtypes of each of eight *glossy* genes.

Table S6. Results from DE comparisons.

Table S7. GO enrichment of DE genes.

Table S8. GCN modules.

Table S9. Means of Absolute Correlation with *glossy* genes (MAC).

Table S10. GO overrepresented in the 264 DE genes from the turquoise module.

Table S11. ICE results and annotation of TFs.

Table S12. Segregation analysis of the *ems12581* mutation.

Table S13. BSR-Seq experiment of *gl14* mutants of three EMS alleles.

Table S14. List of Sequence Read Archive data sets for GCN analysis.

REFERENCES

Aarts, M.G., Keijzer, C.J., Stiekema, W.J. and Pereira, A. (1995) Molecular characterization of the CER1 gene of *Arabidopsis* involved in epicuticular wax biosynthesis and pollen fertility. *Plant Cell*, **7**, 2115–2127.

Aharoni, A., Dixit, S., Jetter, R., Thoenes, E., van Arkel, G. and Pereira, A. (2004) The SHINE clade of AP2 domain transcription factors activates

wax biosynthesis, alters cuticle properties, and confers drought tolerance when overexpressed in *Arabidopsis*. *Plant Cell*, **16**, 2463–2480.

- Bach, L., Michaelson, L.V., Haslam, R. et al. (2008) The very-long-chain hydroxy fatty acyl-CoA dehydratase PASTICCINO2 is essential and limiting for plant development. *Proc. Natl Acad. Sci. USA*, **105**, 14727–14731.
- Beaudoin, F., Wu, X., Li, F., Haslam, R.P., Markham, J.E., Zheng, H., Napier, J.A. and Kunst, L. (2009) Functional characterization of the *Arabidopsis* beta-ketoacyl-coenzyme A reductase candidates of the fatty acid elongase. *Plant Physiol.* **150**, 1174–1191.
- Benjamini, Y. and Hochberg, Y. (1995) Controlling the false discovery rate – a practical and powerful approach to multiple testing. *J. R. Stat. Soc. Series B Stat. Method*, **57**, 289–300.
- Benjamini, Y. and Yekutieli, D. (2001) The control of the false discovery rate in multiple testing under dependency. *Ann. Stat.* **29**, 1165–1188.
- Bernard, A. and Joubes, J. (2013) *Arabidopsis* cuticular waxes: advances in synthesis, export and regulation. *Prog. Lipid Res.* **52**, 110–129.
- Bird, D., Beisson, F., Brigham, A., Shin, J., Greer, S., Jetter, R., Kunst, L., Wu, X., Yephremov, A. and Samuels, L. (2007) Characterization of *Arabidopsis* ABCG11/WBC11, an ATP binding cassette (ABC) transporter that is required for cuticular lipid secretion: WBC11 is required for cuticular lipid transport. *Plant J.* **52**, 485–498.
- Bolger, A.M., Lohse, M. and Usadel, B. (2014) Trimmomatic: a flexible trimmer for Illumina sequence data. *Bioinformatics*, **30**, 2114–2120.
- Broun, P., Poindexter, P., Osborne, E., Jiang, C.Z. and Riechmann, J.L. (2004) WIN1, a transcriptional activator of epidermal wax accumulation in *Arabidopsis*. *Proc. Natl Acad. Sci. USA*, **101**, 4706–4711.
- Chen, W., Yu, X.H., Zhang, K., Shi, J., De Oliveira, S., Schreiber, L., Shanklin, J. and Zhang, D. (2011) Male Sterile2 encodes a plastid-localized fatty acyl carrier protein reductase required for pollen exine development in *Arabidopsis*. *Plant Physiol.* **157**, 842–853.
- Chun, H. and Keles, S. (2010) Sparse partial least squares regression for simultaneous dimension reduction and variable selection. *J. R. Stat. Soc. Series B Stat. Method*, **72**, 3–25.
- Cingolani, P., Platts, A., Le Wang, L., Coon, M., Nguyen, T., Wang, L., Land, S.J., Lu, X. and Ruden, D.M. (2012) A program for annotating and predicting the effects of single nucleotide polymorphisms, SnpEff: SNPs in the genome of *Drosophila melanogaster* strain w1118; iso-2; iso-3. *Fly*, **6**, 80–92.
- De Bigault Du Granrut, A. and Cacas, J.L. (2016) How very-long-chain fatty acids could signal stressful conditions in plants? *Front. Plant Sci.* **7**, 1490.
- Dietrich, C.R. (2002) Molecular and genetic characterization of genes involved in maize cuticular wax biosynthesis. In *Agronomy. Retrospective Theses and Dissertations*. Iowa State University.
- Dietrich, C.R., Perera, M.A., D Yandean-Nelso, M., Meeley, R.B., Nikolau, B.J. and Schnable, P.S. (2005) Characterization of two GL8 paralogs reveals that the 3-ketoacyl reductase component of fatty acid elongase is essential for maize (*Zea mays* L.) development. *Plant J.* **42**, 844–861.
- Dobin, A., Davis, C.A., Schlesinger, F., Drenkow, J., Zaleski, C., Jha, S., Batut, P., Chaisson, M. and Gingeras, T.R. (2013) STAR: ultrafast universal RNA-seq aligner. *Bioinformatics*, **29**, 15–21.
- Fiebig, A., Mayfield, J.A., Miley, N.L., Chau, S., Fischer, R.L. and Preuss, D. (2000) Alterations in CER6, a gene identical to CUT1, differentially affect long-chain lipid content on the surface of pollen and stems. *Plant Cell*, **12**, 2001–2008.
- Gao, C. (2018) The future of CRISPR technologies in agriculture. *Nat. Rev. Mol. Cell Biol.* **19**, 275–276.
- Go, Y.S., Kim, H., Kim, H.J. and Suh, M.C. (2014) *Arabidopsis* cuticular wax biosynthesis is negatively regulated by the DEWAX gene encoding an AP2/ERF-type transcription factor. *Plant Cell*, **26**, 1666–1680.
- Graca, J. (2015) Suberin: the biopolyester at the frontier of plants. *Front. Chem.* **3**, 62.
- Hannoufa, A., Negruk, V., Eisner, G. and Lemieux, B. (1996) The CER3 gene of *Arabidopsis thaliana* is expressed in leaves, stems, roots, flowers and apical meristems. *Plant J.* **10**, 459–467.
- Hansen, J.D., Pyee, J., Xia, Y., Wen, T.J., Robertson, D.S., Kolattukudy, P.E., Nikolau, B.J. and Schnable, P.S. (1997) The *glossy1* locus of maize and an epidermis-specific cDNA from *Kleinia odorata* define a class of receptor-like proteins required for the normal accumulation of cuticular waxes. *Plant Physiol.* **113**, 1091–1100.
- Jenks, M.A., Tuttle, H.A., Eigenbrode, S.D. and Feldmann, K.A. (1995) Leaf epicuticular waxes of the eceriferum mutants in *Arabidopsis*. *Plant Physiol.* **108**, 369–377.

- Jin, J.P., Tian, F., Yang, D.C., Meng, Y.Q., Kong, L., Luo, J.C. and Gao, G. (2017) PlantTFDB 4.0: toward a central hub for transcription factors and regulatory interactions in plants. *Nucleic Acids Res.* **45**, D1040–D1045.
- Kunst, L. and Samuels, A.L. (2003) Biosynthesis and secretion of plant cuticular wax. *Prog. Lipid Res.* **42**, 51–80.
- Langfelder, P. and Horvath, S. (2008) WGCNA: an R package for weighted correlation network analysis. *BMC Bioinformatics*, **9**, 559.
- Lee, S.B. and Suh, M.C. (2013) Recent advances in cuticular wax biosynthesis and its regulation in Arabidopsis. *Mol. Plant*, **6**, 246–249.
- Lee, S.B. and Suh, M.C. (2015) Cuticular wax biosynthesis is up-regulated by the MYB94 transcription factor in Arabidopsis. *Plant Cell Physiol.* **56**, 48–60.
- Lee, S.B., Kim, H., Kim, R.J. and Suh, M.C. (2014) Overexpression of Arabidopsis MYB96 confers drought resistance in *Camelina sativa* via cuticular wax accumulation. *Plant Cell Rep.* **33**, 1535–1546.
- Lee, S.B., Kim, H.U. and Suh, M.C. (2016) MYB94 and MYB96 additively activate cuticular wax biosynthesis in Arabidopsis. *Plant Cell Physiol.* **57**, 2300–2311.
- Li, F., Wu, X., Lam, P., Bird, D., Zheng, H., Samuels, L., Jetter, R. and Kunst, L. (2008) Identification of the wax ester synthase/acyl-coenzyme A: diacylglycerol acyltransferase WSD1 required for stem wax ester biosynthesis in Arabidopsis. *Plant Physiol.* **148**, 97–107.
- Li, L., Li, D., Liu, S. *et al.* (2013) The maize glossy13 gene, cloned via BSR-Seq and Seq-walking encodes a putative ABC transporter required for the normal accumulation of epicuticular waxes. *PLoS ONE*, **8**, e82333.
- Li, L., Du, Y., He, C. *et al.* (2018) A novel maize gene, glossy6 involved in epicuticular wax deposition and drought tolerance. *bioRxiv*, 378687. <https://doi.org/10.1101/378687>.
- Liu, S., Dietrich, C.R. and Schnable, P.S. (2009a) DLA-based strategies for cloning insertion mutants: cloning the gl4 locus of maize using Mu transposon tagged alleles. *Genetics*, **183**, 1215–1225.
- Liu, S., Yeh, C.T., Ji, T., Ying, K., Wu, H., Tang, H.M., Fu, Y., Nettleton, D. and Schnable, P.S. (2009b) Mu transposon insertion sites and meiotic recombination events co-localize with epigenetic marks for open chromatin across the maize genome. *PLoS Genet.* **5**, e1000733.
- Liu, S., Chen, H.D., Makarevitch, I., Shirmer, R., Emrich, S.J., Dietrich, C.R., Barbazuk, W.B., Springer, N.M. and Schnable, P.S. (2010) High-throughput genetic mapping of mutants via quantitative single nucleotide polymorphism typing. *Genetics*, **184**, 19–26.
- Liu, S., Yeh, C.T., Tang, H.M., Nettleton, D. and Schnable, P.S. (2012) Gene mapping via bulked segregant RNA-Seq (BSR-Seq). *PLoS ONE*, **7**, e36406.
- Love, M.I., Huber, W. and Anders, S. (2014) Moderated estimation of fold change and dispersion for RNA-seq data with DESeq2. *Genome Biol.* **15**, 550.
- Lu, S.Y., Song, T., Kosma, D.K., Parsons, E.P., Rowland, O. and Jenks, M.A. (2009) Arabidopsis CER8 encodes LONG-CHAIN ACYL-COA SYNTHETASE 1 (LACS1) that has overlapping functions with LACS2 in plant wax and cutin synthesis. *Plant J.* **59**, 553–564.
- Lu, X., Liu, J., Ren, W. *et al.* (2018) Gene-indexed mutations in maize. *Mol. Plant*, **11**, 496–504.
- McFarlane, H.E., Shin, J.J., Bird, D.A. and Samuels, A.L. (2010) Arabidopsis ABCG transporters, which are required for export of diverse cuticular lipids, dimerize in different combinations. *Plant Cell*, **22**, 3066–3075.
- McKenna, A., Hanna, M., Banks, E. *et al.* (2010) The Genome Analysis Toolkit: a MapReduce framework for analyzing next-generation DNA sequencing data. *Genome Res.* **20**, 1297–1303.
- Moose, S.P. and Sisco, P.H. (1996) Glossy15, an APETALA2-like gene from maize that regulates leaf epidermal cell identity. *Genes Dev.* **10**, 3018–3027.
- Negrjuk, V., Yang, P., Subramanian, M., McNevin, J.P. and Lemieux, B. (1996) Molecular cloning and characterization of the CER2 gene of *Arabidopsis thaliana*. *Plant J.* **9**, 137–145.
- Oshima, Y., Shikata, M., Koyama, T., Ohtsubo, N., Mitsuda, N. and Ohme-Takagi, M. (2013) MIXTA-like transcription factors and WAX INDUCER1/SHINE1 coordinately regulate cuticle development in Arabidopsis and *Torenia fournieri*. *Plant Cell*, **25**, 1609–1624.
- Park, C.S., Go, Y.S. and Suh, M.C. (2016) Cuticular wax biosynthesis is positively regulated by WRINKLED4, an AP2/ERF-type transcription factor, in Arabidopsis stems. *Plant J.* **88**, 257–270.
- Pascal, S., Bernard, A., Sorel, M., Pervent, M., Vile, D., Haslam, R.P., Napier, J.A., Lessire, R., Domergue, F. and Joubes, J. (2013) The Arabidopsis cer26 mutant, like the cer2 mutant, is specifically affected in the very long chain fatty acid elongation process. *Plant J.* **73**, 733–746.
- Pighin, J.A., Zheng, H., Balakshin, L.J., Goodman, I.P., Western, T.L., Jetter, R., Kunst, L. and Samuels, A.L. (2004) Plant cuticular lipid export requires an ABC transporter. *Science*, **306**, 702–704.
- Raffaële, S., Vaillau, F., Leger, A., Joubes, J., Miersch, O., Huard, C., Blee, E., Mongrand, S., Domergue, F. and Roby, D. (2008) A MYB transcription factor regulates very-long-chain fatty acid biosynthesis for activation of the hypersensitive cell death response in Arabidopsis. *Plant Cell*, **20**, 752–767.
- Rowland, O., Zheng, H., Hepworth, S.R., Lam, P., Jetter, R. and Kunst, L. (2006) CER4 encodes an alcohol-forming fatty acyl-coenzyme A reductase involved in cuticular wax production in Arabidopsis. *Plant Physiol.* **142**, 866–877.
- Sanchez-Pulido, L., Martin-Belmonte, F., Valencia, A. and Alonso, M.A. (2002) MARVEL: a conserved domain involved in membrane apposition events. *Trends Biochem. Sci.* **27**, 599–601.
- Schnable, P.S., Stinard, P.S., Wen, T.J., Heinen, S., Weber, D., Schneerman, M., Zhang, L., Hansen, J.D. and Nikolau, B.J. (1994) The genetics of cuticular wax biosynthesis. *Maydica*, **39**, 279–287.
- Schnable, P.S., Ware, D., Fulton, R.S. *et al.* (2009) The B73 maize genome: complexity, diversity, and dynamics. *Science*, **326**, 1112–1115.
- Seo, P.J., Lee, S.B., Suh, M.C., Park, M.J., Go, Y.S. and Park, C.M. (2011) The MYB96 transcription factor regulates cuticular wax biosynthesis under drought conditions in Arabidopsis. *Plant Cell*, **23**, 1138–1152.
- Settles, A.M., Holding, D.R., Tan, B.C. *et al.* (2007) Sequence-indexed mutations in maize using the UniformMu transposon-tagging population. *BMC Genomics*, **8**, 116.
- Sprague, G.F. (1990) Glossies. *Maize Genet. Coop. News Lett.* **64**, 110.
- Tacke, E., Korfhage, C., Michel, D., Maddaloni, M., Motto, M., Lanzini, S., Salamini, F. and Doring, H.P. (1995) Transposon tagging of the maize Glossy2 locus with the transposable element En/Spm. *Plant J.* **8**, 907–917.
- Tian, T., Liu, Y., Yan, H., You, Q., Yi, X., Du, Z., Xu, W. and Su, Z. (2017) agriGO v2.0: a GO analysis toolkit for the agricultural community, 2017 update. *Nucleic Acids Res.* **45**, W122–W129.
- Trapnell, C., Williams, B.A., Pertea, G., Mortazavi, A., Kwan, G., van Baren, M.J., Salzberg, S.L., Wold, B.J. and Pachter, L. (2010) Transcript assembly and quantification by RNA-Seq reveals unannotated transcripts and isoform switching during cell differentiation. *Nat. Biotechnol.* **28**, 511–515.
- Wei, H.R., Persson, S., Mehta, T., Srinivasasainagendra, V., Chen, L., Page, G.P., Somerville, C. and Loraine, A. (2006) Transcriptional coordination of the metabolic network in Arabidopsis. *Plant Physiol.* **142**, 762–774.
- Xia, Y., Nikolau, B.J. and Schnable, P.S. (1996) Cloning and characterization of CER2, an Arabidopsis gene that affects cuticular wax accumulation. *Plant Cell*, **8**, 1291–1304.
- Xu, X., Dietrich, C.R., Delledonne, M., Xia, Y., Wen, T.J., Robertson, D.S., Nikolau, B.J. and Schnable, P.S. (1997) Sequence analysis of the cloned glossy8 gene of maize suggests that it may code for a beta-ketoacyl reductase required for the biosynthesis of cuticular waxes. *Plant Physiol.* **115**, 501–510.
- Young, M.D., Wakefield, M.J., Smyth, G.K. and Oshlack, A. (2010) Gene ontology analysis for RNA-seq: accounting for selection bias. *Genome biology*, **11**, R14.
- Zheng, H., Rowland, O. and Kunst, L. (2005) Disruptions of the Arabidopsis Enoyl-CoA reductase gene reveal an essential role for very-long-chain fatty acid synthesis in cell expansion during plant morphogenesis. *Plant Cell*, **17**, 1467–1481.